Kaposi's sarcoma associated herpesvirus-encoded viral FLICE inhibitory protein (vFLIP) K13 suppresses CXCR4 expression by upregulating miR-146a

Vasu Punj[*], **Hittu Matta**[*], **Sandra Schamus**, **Aletheia Tamewitz**, **Bean Anyang**, and **Preet M. Chaudhary**[‡]

Department of Medicine, Division of Hematology-Oncology, Hillman Cancer Center, University of Pittsburgh Cancer Institute, University of Pittsburgh, Pittsburgh, PA, U.S.A.

Abstract

Kaposi's sarcoma (KS) associated herpesvirus (KSHV)-encoded viral FLICE inhibitory protein (vFLIP) K13 is a potent activator of the NF-κB pathway. Here we demonstrate that infection with KHSV and ectopic expression of K13, but not its NF-κB-defective mutant, suppressed the expression of CXCR4. Suppression of CXCR4 by KSHV and K13 was associated with upregulated expression of miR-146a, a microRNA that is known to bind to the 3′ untranslated region of CXCR4 mRNA. Reporter studies identified two NF-κB sites in the promoter of miR-146a that were essential for its activation by K13. Accordingly, ectopic expression of K13, but not its NF-κB-defective mutant or other vFLIPs, strongly stimulated the miR-146a promoter activity, which could be blocked by specific genetic and pharmacological inhibitors of the NF-κB pathway. Finally, expression of CXCR4 was downregulated in clinical samples of KS and this was accompanied by increased expression of miR-146a. Our results demonstrate that K13-induced NF-κB activity suppresses CXCR4 via upregulation of miR-146a. Downregulation of CXCR4 expression by K13 may contribute to KS development by promoting premature release of KSHV-infected endothelial progenitors into the circulation.

Keywords

KSHV; vFLIP; K13; NF-κB; CXCR4; mir-146a; PEL; HHV8

Introduction

Kaposi's sarcoma (KS)-associated herpesvirus (KSHV), also known as human herpesvirus 8 (HHV-8), is an oncogenic γ2 herpesvirus that was originally identified in KS lesions obtained from HIV-infected individuals (Chang *et al.*, 1994), and has been subsequently

[‡]To whom correspondence and reprint requests should be addressed at the Hillman Cancer Center, 5117 Centre Avenue, Suite 1.19A, Pittsburgh, PA, 15213-1863, Ph: 412-623-7703, Fax: 412-623-1415.
[*]These authors contributed equally to this work.

Conflict of interest
The authors declare no conflict of interest.

etiologically linked to all clinico-epidemiological forms of KS (Dourmishev *et al.*, 2003). In addition to KS, KSHV infection has been associated with primary effusion lymphoma (PEL) and some aggressive forms of multicentric Castleman's disease (Moore and Chang, 2001).

KSHV frequently establishes a latent infection in the target cells, which is characterized by the persistence of the viral genome in the nucleus, and expression of a limited number of viral genes (Dourmishev *et al.*, 2003; Sarid *et al.*, 1998). The three major viral proteins that are expressed during latency include LANA (latency-associated nuclear antigen), v-Cyclin, and K13 (Chaudhary and Nicholas, 2008). The K13 protein resembles the prodomain of caspase 8/FLICE in its structure and was originally classified as a viral FLICE inhibitory protein (vFLIP) (Schulz, 2000; Thome *et al.*, 1997). However, subsequent work has revealed that K13 does not act as an inhibitor of caspase 8, and instead interacts with a multi-subunit Ikappa kinase (IKK) complex to activate the NF-κB pathway (Chaudhary *et al.*, 1999; Chugh *et al.*, 2005; Liu *et al.*, 2002; Matta and Chaudhary, 2004; Matta *et al.*, 2007a; Matta *et al.*, 2003). By hijacking the NF-κB pathway, K13 blocks lytic replication of KSHV, and manipulates diverse cellular processes that regulate cellular survival, proliferation, and cytokine secretion, thereby contributing to cellular transformation and tumorigenesis.(Chugh *et al.*, 2005; Guasparri *et al.*, 2004; Sun *et al.*, 2003a; Sun *et al.*, 2006; Sun *et al.*, 2003b; Xu and Ganem, 2007; Ye *et al.*, 2008; Zhao *et al.*, 2007)

Infection of micro- and macro-vascular endothelial cells with KSHV *in vitro* results in their acquisition of a spindle cell phenotype resembling the spindle cells characteristic of KS lesions (Ciufo *et al.*, 2001; Flore *et al.*, 1998; Moses *et al.*, 1999). We and others recently demonstrated that ectopic expression of K13 in vascular endothelial cells is sufficient to recapitulate this effect of KSHV-infection on spindle cell transformation (Grossmann *et al.*, 2006; Matta *et al.*, 2007b). Furthermore, both KSHV infection and ectopic K13 expression resulted in the upregulated expression of several genes that are known to be involved in the regulation of immune and inflammatory responses, apoptosis, and angiogenesis, and have been implicated in the pathogenesis of KS lesions (Grossmann *et al.*, 2006; Matta *et al.*, 2007b; Naranatt *et al.*, 2004; Poole *et al.*, 2002; Punj *et al.*, 2009a; Punj *et al.*, 2009b; Raggo *et al.*, 2005; Sakakibara *et al.*, 2009; Thurau *et al.*, 2009). In particular, RDC1/CXCR7, a G-protein coupled receptor, was one of most strongly induced transcripts in KSHV-infected vascular endothelial cells (Moses *et al.*, 2002; Poole *et al.*, 2002; Raggo *et al.*, 2005), and was shown to play a key role in their increased proliferation and transformation (Raggo *et al.*, 2005). Strong upregulation of RDC1/CXCR7 was also observed in human vascular endothelial cells upon ectopic expression of K13 (Matta *et al.*, 2007b).

Although RDC-1/CXCR7 was originally labeled an orphan chemokine receptor, it was recently revealed that the principal chemokine ligand for RDC-1/CXCR7 is CXCL12/SDF-1, which also binds CXCR4 (Balabanian *et al.*, 2005; Burns *et al.*, 2006; Sierro *et al.*, 2007). Based on the importance of CXCR4 in CXCL12/SDF-1-induced signaling through RDC-1/CXCR7, we decided to examine the effect of KSHV infection on CXCR4 expression. We report that, in contrast to the situation with *RDC-1/CXCR7*, KSHV infection downregulates CXCR4 gene expression through a novel mechanism that involves K13-induced upregulation of miR-146a, a microRNA that was recently shown to suppress CXCR4 expression by binding to the 3′ UTR of its mRNA (Labbaye *et al.*, 2008). As

CXCR4 plays a key role in the retention of immature cells in the marrow, its downregulation may contribute to KS development by promoting premature release of KSHV-infected progenitors into the circulation.

Materials and Methods

Cell Lines and Reagents

Human Umbilical Vein Endothelial Cells (HUVEC) were purchased from Cambrex (East Rutherford, NJ), and were grown in EMB medium containing 10% FBS (fetal bovine serum) and supplemented with the bullet kit. Cells were used for experiments at passages 2 to 6. HUVECs stably expressing 4-Hydroxytamoxifen (4OHT)-inducible K13-ER^{TAM} have been described previously.(Matta *et al.*, 2007b) 293T, HeLa and K562 cells were obtained from the American Type Culture Collection. SLK cells were kindly provided by Dr. Parkash Gill (University of Southern California). MSCV-based retroviral vectors expressing K13-ER^{TAM} K13-58AAA-ER^{TAM} have been described previously (Matta *et al.*, 2007b; Sun *et al.*, 2003b; Zhao *et al.*, 2007), and were used to generate polyclonal populations of infected cells after selection with G418. Bay-11-7082 and IKK-inhibitor VI [(5-Phenyl-2-ureido) thiophene-3-carboxamide] were purchased from Calbiochem (Gibbstown, NJ). Arsenic trioxide (As$_2$O$_3$) was from Sigma (St. Louis; MO). Rabbit polyclonal antibody against CXCR4 was obtained from NIH AIDS Research and Reference Reagent Program (Rockville, MD). Antibodies against Flag and Tubulin were from Sigma (St. Louis, MO).

Plasmids

Plasmids encoding various vFLIPs and phosphorylation-resistant mutants of IκBα have been described previously (Sun *et al.*, 2006; Sun *et al.*, 2003b). The CXCR4 reporter construct containing a Rous Sarcoma Virus-promoter driven firefly luciferase gene fused to ∼500 bp of the 3′ UTR from CXCR4 mRNA containing its two miR-146a binding sites was cloned in our laboratory. A CXCR4 reporter construct containing mutations in the two of the miR-146a binding sites (site2 and 3) was generated by site directed mutagenesis as described previously (Labbaye *et al.*, 2008). The wild type and mutant miR-146 promoter luciferase reporter constructs were kindly provided by Dr. David Baltimore (California Institute of Technology, Pasadena, CA).

Luciferase Reporter Assay

293 cells were transfected in a 24-well plate with various test plasmids along with the wild-type or mutant miR-146a luciferase reporter constructs or CXCR4 luciferase reporter construct (75 ng/well) and a pRSV/LacZ (β-galactosidase) reporter construct (75 ng/well), using calcium phosphate as described previously (Chaudhary *et al.*, 1999). Cells were lysed 24–36 h later, and extracts were used for the measurement of firefly luciferase and β-galactosidase activities, respectively. Luciferase activity was normalized relative to the β-galactosidase activity to control for the difference in the transfection efficiency. Luciferase reporter assay in HeLa and SLK cells was conducted using Lipofectamine transfection essentially as described previously (Matta *et al.*, 2003).

TaqMan Quantitative Real-time PCR analysis of mature micro-RNA (miR)

Total RNA was isolated using the miRNeasy Mini kit (Qiagen) and *miR-146a* expression was studied, using TaqMan microRNA pre-designed assay as recommended by manufacturer (Applied Biosystems, Inc., Foster City, CA). The assay includes two steps: generation of cDNA followed by TaqMan real time PCR. Briefly, total RNA was reverse-transcribed, using TaqMan miRNA Reverse Transcription Kit following the manufacturer's protocol (Applied Biosystems, Inc., Foster City, CA). TaqMan miRNA assay included specific RT Primers and TaqMan Probes to quantify mature hsa-miR-146a (P/N 4373132). For normalization, hsa-miR-RNU48 (P/N 4373883) was used. All reactions were incubated in a 96-well plate at 95°C for 10 min followed by 40 cycles of 95°C for 15 sec followed by 60°C for 1 min in ABI 7700 system (Applied Biosystems, Inc., Foster City, CA). Melt curve analysis was performed at the end of each qPCR run. No-template and no-reverse transcriptase controls were included. hsa-miR-RNU24 (P/N 4373379) was used as a negative control in the PCR. A threshold cycle (CT) was observed in the exponential phase amplification, and quantification of relative expression levels was performed, using standard curve for target genes and endogenous control generated by a SDS-gel quantification software (Applied Biosystems, Inc. Foster City, CA). An efficiency of 90-100% of PCR was only taken into consideration and mean CT±SE (CT value of target gene-CT value of normalizer) for each target was calculated as described previously (Dorak, 2006; Williams *et al.*, 2007). Therefore higher CT indicates lower expression of target gene.

Real time quantitative PCR for CXCR4 and IL8

Total RNA was isolated, using the RNeasy Mini kit (Qiagen), and quantitative RT-PCR performed as described previously (Zhao *et al.*, 2007). The real-time PCR reactions were performed in triplicate, using an ABI Prism 7700 system and SYBR green-Taq polymerase mix to determine the relative change in the expression of target gene. *Actin* was used as a housekeeping control. CT was calculated for each target as described above. Primers used for real-time PCR are CXCR4 Forward (GCCTTATCCTGCCTGGTATTGTC), CXCR4 Reverse (GCGAAGAAAGCCAGGATGAGGAT), *IL8* Forward (GCCAACACAGAAATTATTGTAAAGCTT), *IL8* Reverse (CCTCTGCACCCAGTTTTCCTT), β-*Actin* Forward (TCACCCACACTGTGCCCATCTACGA), β-*Actin* Reverse (CAGCGGAACCGCTCATTGCCAATGG).

Statistical Analysis

Data is expressed as mean CT±SE unless otherwise indicated. Student's t- test (Unpaired, two tailed) was used to determine the differential expression of *miR-146a* and *CXCR4* and P value (*P<0.05 and ** P<0.01) was calculated in Graph Pad Prism 5.02 (Graph Pad software, La Jolla). Scatter plot for expression of miR-146a and CXCR4 in patient samples was plotted using Graph Pad Prism 5.02 software.

Results

KSHV downregulates CXCR4 expression in vascular endothelial cells

To examine the effect of KSHV infection on CXCR4 expression we utilized the publicly accessible Gene Expression Omnibus (GEO) datasets. We used Gene Spring GX10 (Agilent Technology) software to reanalyze a dataset of Affymetrix GeneChip expression analysis (Dataset Record GDS940) and observed 2.5 fold downregulation of CXCR4 expression in primary human dermal endothelial cells (HDMEC) that had been infected with KSHV as compared to the uninfected control cells.

To confirm the GeneChip results, we infected telomerase-immortalized human vascular endothelial cells (iHUVECs) with KSHV, and examined the expression of CXCR4 by qRT-PCR and immunoblot analyses. The relative expression is presented as ∆CT values (CT value of target gene minus CT value of house-keeping gene *actin*), therefore the smaller ∆CT values represent higher gene expression. As shown in Figure 1a-b, we observed significant downregulation of CXCR4 mRNA expression in iHUVECs that had been infected with KSHV for 12- 94 h, and this was accompanied by a parallel reduction in the level of the CXCR4 protein.

K13 mimics the effect of KSHV infection on CXCR4 downregulation

K13 is one of the few KSHV-encoded proteins to be expressed in cells latently infected with the virus. As such, we next examined whether K13 can mimic the effect of KSHV infection on CXCR4 expression in vascular endothelial cells. For this purpose, we used HUVECs stably expressing a K13-ER^{TAM} fusion construct, in which the K13 cDNA is fused in-frame to the ligand-binding domain of a mutated estrogen receptor (Matta *et al.*, 2007b). The mutated estrogen receptor encoded by this fusion construct does not bind to its physiological ligand estrogen, but binds with very high affinity to the synthetic ligand 4OHT (4-hydroxytamoxifen), and allows control of K13-induced NF-κB activity in a 4OHT-dependent fashion (Matta *et al.*, 2007a). To examine the effect of K13 on CXCR4 expression, we treated the HUVECs-K13-ER^{TAM} and HUVECs-vector with 4OHT and examined the effect of the treatment on CXCR4 expression by qRT-PCR and immunoblot analyses. As shown in Figure 2a, there was a significant difference (*P<0.05) in the mean ∆CT values of 4OHT-treated HUVECs-K13-ER^{TAM} as compared to untreated cells suggesting a significant down-regulation of CXCR4 mRNA. This was accompanied by a reduction in the CXCR4 protein expression (Figure 2b). Treatment with 4OHT had no significant effect on CXCR4 mRNA or protein level in the HUVECs-vector (Figure 2a-b). In contrast to the situation with CXCR4, the ∆CT value for IL-8 in the 4OHT-treated K13-ER^{TAM} cells was significantly lower (*P<0.01) as compared to the untreated cells, indicating an upregulation of IL-8 expression (Figure 2c), indicating that the effect of K13 on CXCR4 downregulation is specific. To rule out the possibility that the observed downregulation of CXCR4 expression in HUVECs was an indirect consequence of spindle cell differentiation that accompanies induction of K13 activity (Matta *et al.*, 2007b), we examined the effect 4OHT on CXCR4 expression in K13-ER^{TAM}-expressing K562 (Chronic Myeloid Leukemia) cells. Similar to the situation with HUVECs, 4OHT

downregulated CXCR4 expression at the mRNA and protein levels in the K562-K13-ER^{TAM} cells, but upregulated IL-8 expression (Figure 2d-f).

KSHV- and K13-induced downregulation of CXCR4 expression is associated with increased miR-146a expression

A recent study demonstrated that miR-146a downregulates the expression of CXCR4 in K562 cells by binding to two sites in its 3′UTR (Labbaye *et al.*, 2008). To examine the hypothesis that KSHV might suppress CXCR4 expression via miR-146a, we used qRT-PCR analysis to examine the effect of KSHV infection on miR-146a expression in HUVECs. We observed a significant upregulation of miR-146a expression in HUVECs at 6, 12, and 48 h after KSHV infection, as reflected by decline in the corresponding CT values (Figure 3a).

We next asked whether K13 could mimic the effect of KSHV on miR-146a upregulation in HUVECs. As shown in Figure 3b-c, 4OHT treatment resulted in robust (**P<0.01) upregulation of miR-146a expression in the K13-ER^{TAM}-expressing HUVECs and K562 cells, respectively, but was without effect in the corresponding control vector-expressing cells. 4OHT treatment had no significant effect on the expression of miR-RNU24, a house keeping microRNA (Figure 3b-c). Thus, ectopic expression of K13 is sufficient to induce miR-146a expression in cells of different lineage and this effect is not limited to cells infected with KSHV.

Ectopic miR-146a expression downregulates CXCR4 in HUVECs

In the case K13 downregulates CXCR4 gene expression by upregulating miR-146a, ectopic expression of miR-146a should be expected to do the same. To test this hypothesis, we used lentiviral-mediated gene transfer to generate stable clones of HUVECs expressing miR146. We confirmed the increased expression of miR-146a in the stably transduced cells by qRT-PCR analysis (Figure 3d). Subsequently, we examined the effect of ectopic miR-146a expression on CXCR4 gene expression. As shown in Figure 3e, we observed significant downregulation (*P<0.05) of CXCR4 mRNA expression (reflected by higher CT) in the miR-146a-expressing HUVECs as compared to the empty vector-expressing cells.

K13 stimulates miR-146a promoter activity via NF-κB activation

K13 is a potent activator of the NF-κB pathway (Chaudhary *et al.*, 1999). To examine whether the NF-κB pathway is also involved in K13-induced miR-146a upregulation, we took advantage of a previously described K13 mutant, K13-58AAA, which lacks the ability to activate the NF-κB pathway (Sun *et al.*, 2003b). We generated stable clones of HeLa expressing an empty vector, K13-ER^{TAM} and K13-58AAA-ER^{TAM} constructs, and used a luciferase-based reporter assay to examine their ability to activate NF-κB in response to 4OHT. Consistent with our previously reported results, 4OHT resulted in robust NF-κB activation in the HeLa-K13-ER^{TAM} cells, but failed to do so in the K13-58AAA-ER^{TAM} cells (Figure 4a). More importantly, 4OHT resulted in significant (*P<0.05) upregulation of miR-146a expression in the HeLa-K13-ER^{TAM} cells (reflected by lower CT), but not in the HeLa-vector or HeLa-K13-58AAA-ER^{TAM} cells (Figure 4b), thereby implicating the NF-κB pathway in this process.

To confirm the above results and to further examine the mechanism by which K13 upregulates miR-146a, we transfected 293T cells with a luciferase-based reporter construct containing the miR-146a promoter region (miR-146a-WT-Luc). Coexpression of K13 led to a significant increase in miR-146a-Luc activity, whereas coexpresssion of K13-58AAA failed to do so (Figure 4c). Furthermore, no miR-146a promoter activation was observed upon coexpression of vFLIP E8 from the equine herpesvirus 2, and vFLIPs MC159 and MC160 from the molluscum contagiosum virus, which resemble K13 in structure but lack the ability to activate the NF-κB pathway (Chaudhary *et al.*, 1999; Matta *et al.*, 2008) (Figure 4d). On the other hand, coexpression of Human T-cell Leukemia-encoded Tax protein, which resembles K13 in activating the NF-κB pathway, led to robust miR-146a promoter activation (Figure 4d). Induction of miR-146a promoter activity by K13, however, was not limited to 293T cells. Treatment of K13-ER^{TAM}–transfected SLK (a KS-derived cell line) cells with 4OHT resulted in significant activation of NF-κB-Luc and miR-146a-Luc reporter constructs (Figure 4e-f). Collectively, these results indicate that K13 upregulates miR-146a expression primarily through activation of its transcription via an NF-κB-dependent mechanism.

The NF-κB sites in the miR-146a promoter are essential for K13-mediated activation

The miR-146a promoter region contains two NF-κB binding-elements (Taganov *et al.*, 2006). To examine the involvement of these κB sites in K13-induced miR-146a upregulation, we transiently transfected 293T cells with either a luciferase reporter construct containing the wild-type miR-146a promoter (miR-146a-WT-Luc) or a reporter construct (miR-146a-NF-κBm2-Luc) with mutations in the κB sites. As shown in Figures 4g, mutation of the two κB sites in the miR-146a-NF-κBm2-Luc construct nearly abolished K13-induced miR-146a promoter activity, confirming the importance of the κB sites in K13-mediated miR-146a upregulation.

Abrogation of K13-induced miR-146a promoter activation by genetic and pharmacological inhibitors of the NF-κB pathway

K13 activates the NF-κB pathway by inducing phosphorylation of IκBα, targeting it for ubiquitination and subsequent degradation via proteasome (Liu *et al.*, 2002). We next examined the effect of two phosphorylation-resistant mutants of IκBα on K13-induced mir-146a promoter activity. As shown in Figure 5a, K13-induced mir-146a promoter activity was completely blocked by either a phosphorylation-resistant mutant of IκBα in which the two critical serine residues have been mutated to alanine (IκBα SS32/36AA), or a deletion mutant of IκBα lacking the N- terminal 36 amino acids (IκBα N).

K13 activates the NF-κB pathway by activating the IKK complex (Chaudhary *et al.*, 1999; Liu *et al.*, 2002). Therefore, we examined whether specific inhibitors of NF-κB and IKK complex can block K13-induced miR-146a promoter activity. As shown in Figure 5b, treatment with Bay-11-7082, a specific inhibitor of NF-κB, and IKK inhibitor VI (Baxter *et al.*, 2004) effectively blocked K13 transactivated miR-146a promoter activity in 293T cells. In addition, arsenic trioxide, a known inhibitor of K13-induced NF-κB (Matta *et al.*, 2003), completely blocked K13-induced miR-146a promoter activity (Figure 5b).

K13 suppresses a CXCR4-3′UTR reporter construct

To provide further support for the hypothesis that the expression of CXCR4 gene is regulated at the post-transcriptional level by K13-induced miR-146a, we used a CXCR4-3′UTR reporter construct. This construct contains a Rous Sarcoma Virus promoter driven firefly luciferase cDNA fused to ∼500 bp of the 3′ UTR from CXCR4 mRNA containing its miR-146a binding sites. We transiently transfected the CXCR4-3′UTR reporter construct in the HeLa-vector, HeLa-K13-ER^{TAM} and HeLa-K13-58AAA-ER^{TAM} cells and studied the effect of 4OHT treatment on the luciferase activity in the cell extracts. As shown in Figure 6a, we observed a significant reduction in the firefly luciferase activity upon 4OHT treatment in the Hela-K13-ER^{TAM} cells but not in the HeLa-vector cells, supporting the argument that CXCR4 mRNA is target of post-transcriptional repression by K13. Treatment with 4OHT had no significant effect on the luciferase activity in the HeLa-K13-58AAA-ER^{TAM} cells (Figure 6a), thereby supporting the role of K13-induced NF-κB activity in this process.

The CXCR4 3′UTR contains three sites complementary to miR-146a. Of these, sites 2 and 3 are functionally involved in the suppression of CXCR4 by miR-146a (Labbaye *et al.*, 2008). To confirm that K13 suppresses CXCR4 gene expression via miR-146a, we generated a CXCR4-3′UTR reporter construct containing mutations in the miR-146a binding sites 2 and 3. We transfected the wild-type and mutant CXCR4-3′UTR reporter constructs in HeLa-K13-ER^{TAM} cells. Consistent with previous results, 4OHT treatment led to significant reduction in the luciferase activity in the cells transfected with the wild-type construct, but not in those transfected with the mutant construct (Figure 6b). Essentially similar results were obtained when the experiment was repeated in the SLK cells (Figure 6c). Finally, infection of iHUVECs with KSHV effectively blocked the wild-type CXCR4-3′UTR reporter activity but had no significant effect on the mutant CXCR4-3′UTR reporter activity (Figure 6d). Taken collectively, the above results demonstrate that KSHV and K13 downregulate CXCR4 expression by upregulating miR-146a.

Increased miR-146a and decreased *CXCR4* expression in KS clinical specimens

To determine the clinical significance of our results, we examined the expression of miR-146a and CXCR4 in KS (n= 6) and normal skin (n=10) samples by quantitative RT-PCR analysis. As shown in Figure 7, the mean CT values for miR-146a of six KS samples (6.70±1.12) were significantly (**P<0.01) lower than mean CT values for normal skin samples (12.21±0.97) suggesting a significant higher expression of miR-146a in the KS samples. On the contrary, CT for CXCR4 for KS samples was significantly higher (11.04± 0.848) than normal skin samples (7.99± 0.566), thereby indicating a significant (* P<0.05) downregulation of CXCR4 expression in KS skin samples. Taken collectively, these results suggest that KSHV-mediated upregulation of *miR-146a* and downregulation of *CXCR4* that we demonstrated *in vitro* also occur *in vivo*.

Discussion

Infection of vascular endothelial cells with KSHV is known to upregulate the expression of several cytokines, chemokines and chemokine receptors (Moses *et al.*, 2002; Naranatt *et al.*,

2004; Poole *et al.*, 2002; Raggo *et al.*, 2005). In particular, the gene for RDC-1/CXCR7, one of the receptors of CXCL12/SDF-1, is one of the most upregulated genes in KSHV-infected vascular endothelial cells (Moses *et al.*, 2002; Poole *et al.*, 2002; Raggo *et al.*, 2005). In this report, we demonstrate that in contrast to RDC-1/CXCR7, the expression of CXCR4, the other known receptor of CXCL12/SDF-1, is significantly downregulated by KSHV infection. We and others had previously shown that ectopic expression of K13 is sufficient to mimic the effect of KSHV infection on spindle cell transformation and RDC-1/CXCR7 upregulation (Grossmann *et al.*, 2006; Matta *et al.*, 2007b). Consistent with these results, we demonstrate here that expression of K13 is also sufficient to downregulate CXCR4 expression in HUVECs. Since K13 is one of the few KSHV-encoded proteins to be expressed in latently-infected endothelial cells, our results suggest its major role in the downregulation of CXCR4 expression by KSHV, although a contribution of other KSHV-encoded proteins in this process can not be entirely ruled out.

To delineate the mechanism of CXCR4 suppression by KSHV, we focused on miR-146a, as it was reported recently that miR-146a could suppress CXCR4 expression by binding to the 3′UTR of the latter mRNA (Labbaye *et al.*, 2008). The involvement of miR-146a in KSHV- and K13-induced CXCR4 suppression is supported by the following data. *First*, we observed significant upregulation of miR-146a in HUVECs upon infection with KSHV and upon induction of K13 activity. *Second*, ectopic expression of miR-146a resulted in significant downregulation of CXCR4 expression. *Finally*, infection with KSHV or ectopic expression of K13 suppressed the wild-type CXCR4-3′UTR reporter but had no effect on a CXCR4-3′UTR reporter containing mutations in the miR-146a-binding sites. Taken collectively, the above results support the hypothesis that KSHV and K13 suppress CXCR4 by upregulating miR-146a expression.

Previous studies have characterized the mechanism of miR-146a induction by inflammatory stimuli and viral infections (Cameron *et al.*, 2008; Taganov *et al.*, 2006; Williams *et al.*, 2008). Although the miR-146a promoter contains binding sites for several transcription factors, two NF-κB binding sites have been shown to be primarily responsible for its induction by lipopolysaccharide and EBV-encoded latent membrane protein 1 (Cameron *et al.*, 2008; Taganov *et al.*, 2006). Consistent with these earlier reports, our results demonstrate that the NF-κB pathway is also primarily responsible for K13-induced miR-146a induction. This conclusion is supported by the following data. *First*, we observed a strong correlation between the ability of K13 constructs to activate NF-κB and their ability to activate miR-146a promoter. Thus, while the miR-146a promoter was strongly activated by coexpression of wild-type K13, no promoter activation was observed by coexpression of the K13-58AAA mutant that lacks NF-κB activity. Similarly, vFLIPs MC159, MC160 and E8, which lack NF-κB activity, failed to activate the miR-146a promoter, while HTLV1-encoded Tax, a known NF-κB activator, successfully activated it. *Second*, K13 failed to activate a miR-146a promoter that carried mutations in the two NF-κB binding sites. *Finally*, K13-induced miR-146a promoter activity was blocked by genetic (i.e. IκBα SS32/36AA and NIκBα) and chemical (i.e. Bay-11-7082, IKK inhibitors VI, and arsenic trioxide) inhibitors of the NF-κB pathway.

What is the biological significance of CXCR4 downregulation by KSHV? Recent studies suggest that new blood vessels in tumors develop not only from existing vessels, but also from circulating endothelial progenitor cells originating from the bone marrow (Ahn and Brown, 2009). CXCR4 is highly expressed on immature cells, including endothelial progenitors, in bone marrow and its most important function is believed to retain them in the marrow for their further maturation (Urbich and Dimmeler, 2004). Downregulation of CXCR4 may result in premature release of KSHV-infected endothelial progenitors into circulation, which may subsequently home to the permissive sites and propagate to produce KS lesions. Support for the above hypothesis is provided by a recent study that reported evidence of KSHV infection in the circulating endothelial cells in patients with KS (Pellet *et al.*, 2006). Although CXCL12/SDF-1 binds to both CXCR4 and RDC-1/CXCR7, it does not induce signaling through RDC-1/CXCR7 (Balabanian *et al.*, 2005; Burns *et al.*, 2006; Sierro *et al.*, 2007). Instead, RDC-1/CXCR7 forms a functional heterodimer with CXCR4 and enhances CXCL12/SDF-1-induced signaling (Sierro *et al.*, 2007). Therefore, future studies should also examine the possibility that suppression of CXCR4 by KSHV may represent a regulatory mechanism to modulate signaling through CXCL12/SDF-1.

Based on current estimates, any given miRNA can regulate >100 targets. miR-146a has been also implicated in the regulation of genes involved in immune and inflammatory responses (Williams *et al.*, 2008). Thus, Taganov *et al* reported that miR-146a "fine-tunes" the innate immune response by downregulating the expression of IRAK1 and TRAF6, two proteins involved in TLR-signaling pathway (Taganov *et al.*, 2006). miR-146a is also rapidly induced following cellular treatment with IL-1β, and negatively regulates the release of proinflammatory cytokines IL8 and RANTES, which has led to the suggestion that miR-146a might represent a negative feedback mechanism to control the severity of the inflammatory response (Perry *et al.*, 2008). Interestingly, miR-146a expression is also highly induced in cells latently infected with the Epstein-Barr Virus due to the activity of EBV-encoded latent membrane protein 1 (LMP1) (Cameron *et al.*, 2008; Motsch *et al.*, 2007). Furthermore, ectopic expression of miR-146a has been shown to downregulate the expression of a number of interferon-responsive genes, suggesting that miR-146a may functions in a negative feedback loop to modulate the intensity and/or duration of the interferon response (Cameron *et al.*, 2008). Thus, K13 and KSHV-induced miR-146a upregulation may have a broad effect on gene expression and additional studies are needed to delineate fully its role in the regulation of immune and inflammatory responses during the natural history of KSHV infection and in the pathogenesis of KSHV-associated malignancies.

K13 is one of the few KSHV-encoded proteins to be expressed in cells latently infected with the virus and a key player in the pathogenesis of KSHV-associated malignancies (Chaudhary and Nicholas, 2008). Previous studies have shown that K13-induced NF-κB upregulates the expression of a large number of genes that control cellular survival, proliferation, transformation, and immune and inflammatory responses (Grossmann *et al.*, 2006; Matta *et al.*, 2007b; Punj *et al.*, 2009a; Sakakibara *et al.*, 2009; Thurau *et al.*, 2009). Most of these K13-induced genes, such as IL6, IL8, RANTES, and CCL20, are known targets of the NF-κB pathway, suggesting a direct role of the NF-κB pathway in their

upregulation (Grossmann *et al.*, 2006; Matta *et al.*, 2007b; Punj *et al.*, 2009a Punj *et al.*, 2009b; Sakakibara *et al.*, 2009; Thurau *et al.*, 2009). However, K13 also downregulates the expression of numerous genes (Punj *et al.*, 2009a). Data presented here demonstrates that K13-induced NF-κB upregulates the expression of miR-146a, which may explain, at least in part, how K13 might downregulate the expression of cellular genes. Thus, both the direct and indirect (via miRNAs) effects of K13 on cellular and viral gene expression might contribute to its biological role in the natural history of KSHV infection and in the pathogenesis of KSHV-associated malignancies.

Acknowledgments

References

Ahn GO, Brown JM. Role of endothelial progenitors and other bone marrow-derived cells in the development of the tumor vasculature. Angiogenesis. 2009

Balabanian K, Lagane B, Infantino S, Chow KY, Harriague J, Moepps B, et al. The chemokine SDF-1/ CXCL12 binds to and signals through the orphan receptor RDC1 in T lymphocytes. J Biol Chem. 2005; 280:35760–6. [PubMed: 16107333]

Baxter A, Brough S, Cooper A, Floettmann E, Foster S, Harding C, et al. Hit-to-lead studies: the discovery of potent, orally active, thiophenecarboxamide IKK-2 inhibitors. Bioorg Med Chem Lett. 2004; 14:2817–22. [PubMed: 15125939]

Burns JM, Summers BC, Wang Y, Melikian A, Berahovich R, Miao Z, et al. A novel chemokine receptor for SDF-1 and I-TAC involved in cell survival, cell adhesion, and tumor development. J Exp Med. 2006; 203:2201–13. [PubMed: 16940167]

Cameron JE, Yin Q, Fewell C, Lacey M, McBride J, Wang X, et al. Epstein-Barr virus latent membrane protein 1 induces cellular MicroRNA miR-146a, a modulator of lymphocyte signaling pathways. J Virol. 2008; 82:1946–58. [PubMed: 18057241]

Chang Y, Cesarman E, Pessin MS, Lee F, Culpepper J, Knowles DM, et al. Identification of herpesvirus-like DNA sequences in AIDS-associated Kaposi's sarcoma. Science. 1994; 266:1865–9. [PubMed: 7997879]

Chaudhary PM, Jasmin A, Eby MT, Hood L. Modulation of the NF-kappa B pathway by virally encoded death effector domains-containing proteins. Oncogene. 1999; 18:5738–46. [PubMed: 10523854]

Chaudhary, PM.; Nicholas, J. Molecular Biology of Human Herpesvirus 8 neoplasia. In: Nicholas, J.; Jeang, KT.; Wu, TC., editors. Human Cancer Viruses Principles of Transformation and Pathogenesis. Karger; Basel: 2008. p. 186-210.

Chugh P, Matta H, Schamus S, Zachariah S, Kumar A, Richardson JA, et al. Constitutive NF-kappaB activation, normal Fas-induced apoptosis, and increased incidence of lymphoma in human herpes virus 8 K13 transgenic mice. Proc Natl Acad Sci U S A. 2005; 102:12885–90. [PubMed: 16120683]

Ciufo DM, Cannon JS, Poole LJ, Wu FY, Murray P, Ambinder RF, et al. Spindle cell conversion by Kaposi's sarcoma-associated herpesvirus: formation of colonies and plaques with mixed lytic and latent gene expression in infected primary dermal microvascular endothelial cell cultures. J Virol. 2001; 75:5614–26. [PubMed: 11356969]

Dorak, T. Real Time PCR. Taylor & Francis; 2006. p. 333

Dourmishev LA, Dourmishev AL, Palmeri D, Schwartz RA, Lukac DM. Molecular Genetics of Kaposi's Sarcoma-Associated Herpesvirus (Human Herpesvirus 8) Epidemiology and Pathogenesis. Microbiol Mol Biol Rev. 2003; 67:175–212. [PubMed: 12794189]

Flore O, Rafii S, Ely S, JJ OL, Hyjek EM, Cesarman E. Transformation of primary human endothelial cells by Kaposi's sarcoma- associated herpesvirus. Nature. 1998; 394:588–92. [PubMed: 9707121]

Grossmann C, Podgrabinska S, Skobe M, Ganem D. Activation of NF-kappaB by the latent vFLIP gene of Kaposi's sarcoma-associated herpesvirus is required for the spindle shape of virus-infected endothelial cells and contributes to their proinflammatory phenotype. J Virol. 2006; 80:7179–85. [PubMed: 16809323]

Guasparri I, Keller SA, Cesarman E. KSHV vFLIP is essential for the survival of infected lymphoma cells. J Exp Med. 2004; 199:993–1003. [PubMed: 15067035]

Labbaye C, Spinello I, Quaranta MT, Pelosi E, Pasquini L, Petrucci E, et al. A three-step pathway comprising PLZF/miR-146a/CXCR4 controls megakaryopoiesis. Nat Cell Biol. 2008; 10:788–801. [PubMed: 18568019]

Liu L, Eby MT, Rathore N, Sinha SK, Kumar A, Chaudhary PM. The Human Herpes Virus 8-encoded Viral FLICE Inhibitory Protein Physically Associates with and Persistently Activates the Ikappa B Kinase Complex. J Biol Chem. 2002; 277:13745–51. [PubMed: 11830587]

Matta H, Chaudhary PM. Activation of alternative NF-kappa B pathway by human herpes virus 8-encoded Fas-associated death domain-like IL-1 beta-converting enzyme inhibitory protein (vFLIP). Proc Natl Acad Sci U S A. 2004; 101:9399–404. [PubMed: 15190178]

Matta H, Mazzacurati L, Schamus S, Yang T, Sun Q, Chaudhary PM. Kaposi's Sarcoma-associated Herpesvirus (KSHV) Oncoprotein K13 Bypasses TRAFs and Directly Interacts with the I{kappa}B Kinase Complex to Selectively Activate NF-{kappa}B without JNK Activation. J Biol Chem. 2007a; 282:24858–65. [PubMed: 17597077]

Matta H, Punj V, Schamus S, Mazzacurati L, Chen AM, Song R, et al. A nuclear role for Kaposi's sarcoma-associated herpesvirus-encoded K13 protein in gene regulation. Oncogene. 2008; 27:5243–53. [PubMed: 18469854]

Matta H, Sun Q, Moses G, Chaudhary PM. Molecular genetic analysis of human herpes virus 8-encoded viral FLICE inhibitory protein-induced NF-kappaB activation. Journal of Biological Chemistry. 2003; 278:52406–11. [PubMed: 14561765]

Matta H, Surabhi RM, Zhao J, Punj V, Sun Q, Schamus S, et al. Induction of spindle cell morphology in human vascular endothelial cells by human herpesvirus 8-encoded viral FLICE inhibitory protein K13. Oncogene. 2007b; 26:1656–60. [PubMed: 16936773]

Moore PS, Chang Y. Molecular virology of Kaposi's sarcoma-associated herpesvirus. Philos Trans R Soc Lond B Biol Sci. 2001; 356:499–516. [PubMed: 11313008]

Moses AV, Fish KN, Ruhl R, Smith PP, Strussenberg JG, Zhu L, et al. Long-term infection and transformation of dermal microvascular endothelial cells by human herpesvirus 8. J Virol. 1999; 73:6892–902. [PubMed: 10400787]

Moses AV, Jarvis MA, Raggo C, Bell YC, Ruhl R, Luukkonen BG, et al. Kaposi's sarcoma-associated herpesvirus-induced upregulation of the c-kit proto-oncogene, as identified by gene expression profiling, is essential for the transformation of endothelial cells. J Virol. 2002; 76:8383–99. [PubMed: 12134042]

Motsch N, Pfuhl T, Mrazek J, Barth S, Grasser FA. Epstein-Barr virus-encoded latent membrane protein 1 (LMP1) induces the expression of the cellular microRNA miR-146a. RNA Biol. 2007; 4:131–7. [PubMed: 18347435]

Naranatt PP, Krishnan HH, Svojanovsky SR, Bloomer C, Mathur S, Chandran B. Host gene induction and transcriptional reprogramming in Kaposi's sarcoma-associated herpesvirus (KSHV/HHV-8)-infected endothelial, fibroblast, and B cells: insights into modulation events early during infection. Cancer Res. 2004; 64:72–84. [PubMed: 14729610]

Pellet C, Kerob D, Dupuy A, Carmagnat MV, Mourah S, Podgorniak MP, et al. Kaposi's sarcoma-associated herpesvirus viremia is associated with the progression of classic and endemic Kaposi's sarcoma. J Invest Dermatol. 2006; 126:621–7. [PubMed: 16410791]

Perry MM, Moschos SA, Williams AE, Shepherd NJ, Larner-Svensson HM, Lindsay MA. Rapid changes in microRNA-146a expression negatively regulate the IL-1beta-induced inflammatory response in human lung alveolar epithelial cells. J Immunol. 2008; 180:5689–98. [PubMed: 18390754]

Poole LJ, Yu Y, Kim PS, Zheng QZ, Pevsner J, Hayward GS. Altered patterns of cellular gene expression in dermal microvascular endothelial cells infected with Kaposi's sarcoma-associated herpesvirus. J Virol. 2002; 76:3395–420. [PubMed: 11884566]

Punj V, Matta H, Schamus S, Chaudhary PM. Integrated microarray and multiplex cytokine analyses of Kaposi's Sarcoma Associated Herpesvirus viral FLICE Inhibitory Protein K13 affected genes and cytokines in human blood vascular endothelial cells. BMC Med Genomics. 2009a; 2:50. [PubMed: 19660139]

Punj V, Matta H, Schamus S, Yang T, Chang Y, Chaudhary PM. Induction of CCL20 production by Kaposi's sarcoma-associated herpesvirus: role of viral FLICE inhibitory protein K13-induced NF-{kappa}B activation. Blood. 2009b

Raggo C, Ruhl R, McAllister S, Koon H, Dezube BJ, Fruh K, et al. Novel cellular genes essential for transformation of endothelial cells by Kaposi's sarcoma-associated herpesvirus. Cancer Res. 2005; 65:5084–95. [PubMed: 15958552]

Sakakibara S, Pise-Masison CA, Brady JN, Tosato G. Gene regulation and functional alterations induced by Kaposi's sarcoma-associated herpesvirus-encoded ORFK13/vFLIP in endothelial cells. J Virol. 2009; 83:2140–53. [PubMed: 19091861]

Sarid R, Flore O, Bohenzky RA, Chang Y, Moore PS. Transcription mapping of the Kaposi's sarcoma-associated herpesvirus (human herpesvirus 8) genome in a body cavity-based lymphoma cell line (BC-1). J Virol. 1998; 72:1005–12. [PubMed: 9444993]

Schulz TF. Kaposi's sarcoma-associated herpesvirus (human herpesvirus 8): epidemiology and pathogenesis. J Antimicrob Chemother. 2000; 45(T3):15–27. [PubMed: 10855768]

Sierro F, Biben C, Martinez-Munoz L, Mellado M, Ransohoff RM, Li M, et al. Disrupted cardiac development but normal hematopoiesis in mice deficient in the second CXCL12/SDF-1 receptor, CXCR7. Proc Natl Acad Sci U S A. 2007; 104:14759–64. [PubMed: 17804806]

Sun Q, Matta H, Chaudhary PM. The human herpes virus 8-encoded viral FLICE inhibitory protein protects against growth factor withdrawal-induced apoptosis via NF-kappa B activation. Blood. 2003a; 101:1956–61. [PubMed: 12406869]

Sun Q, Matta H, Lu G, Chaudhary PM. Induction of IL-8 expression by human herpesvirus 8 encoded vFLIP K13 via NF-kappaB activation. Oncogene. 2006; 25:2717–26. [PubMed: 16418726]

Sun Q, Zachariah S, Chaudhary PM. The human herpes virus 8-encoded viral FLICE-inhibitory protein induces cellular transformation via NF-kappaB activation. Journal of Biological Chemistry. 2003b; 278:52437–45. [PubMed: 14563855]

Taganov KD, Boldin MP, Chang KJ, Baltimore D. NF-kappaB-dependent induction of microRNA miR-146, an inhibitor targeted to signaling proteins of innate immune responses. Proc Natl Acad Sci U S A. 2006; 103:12481–6. [PubMed: 16885212]

Thome M, Schneider P, Hofmann K, Fickenscher H, Meinl E, Neipel F, et al. Viral FLICE-inhibitory proteins (FLIPs) prevent apoptosis induced by death receptors. Nature. 1997; 386:517–21. [PubMed: 9087414]

Thurau M, Marquardt G, Gonin-Laurent N, Weinlander K, Naschberger E, Jochmann R, et al. Viral inhibitor of apoptosis vFLIP/K13 protects endothelial cells against superoxide-induced cell death. J Virol. 2009; 83:598–611. [PubMed: 18987137]

Urbich C, Dimmeler S. Endothelial progenitor cells: characterization and role in vascular biology. Circ Res. 2004; 95:343–53. [PubMed: 15321944]

Williams AE, Perry MM, Moschos SA, Larner-Svensson HM, Lindsay MA. Role of miRNA-146a in the regulation of the innate immune response and cancer. Biochem Soc Trans. 2008; 36:1211–5. [PubMed: 19021527]

Williams AE, Perry MM, Moschos SA, Lindsay MA. microRNA expression in the aging mouse lung. BMC Genomics. 2007; 8:172. [PubMed: 17573962]

Xu Y, Ganem D. Induction of chemokine production by latent Kaposi's sarcoma-associated herpesvirus infection of endothelial cells. J Gen Virol. 2007; 88:46–50. [PubMed: 17170435]

Ye FC, Zhou FC, Xie JP, Kang T, Greene W, Kuhne K, et al. Kaposi's sarcoma-associated herpesvirus latent gene vFLIP inhibits viral lytic replication through NF-kappaB-mediated suppression of the AP-1 pathway: a novel mechanism of virus control of latency. J Virol. 2008; 82:4235–49. [PubMed: 18305042]

Zhao J, Punj V, Matta H, Mazzacurati L, Schamus S, Yang Y, et al. K13 Blocks KSHV Lytic Replication and Deregulates vIL6 and hIL6 Expression: a Model of Lytic Replication Induced Clonal Selection in Viral Oncogenesis. PLoS ONE. 2007; 2:e1067. [PubMed: 17957251]
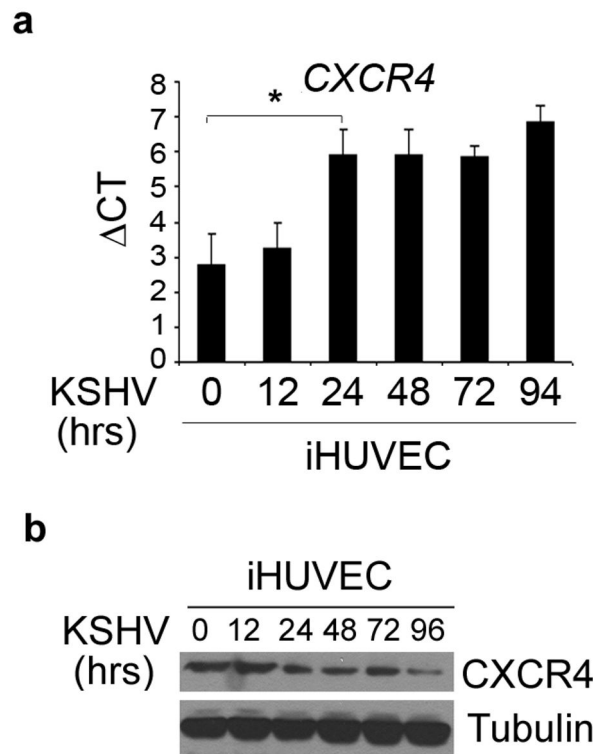
a

b

Figure 1. KSHV downregulates CXCR4 expression in vascular endothelial cells
a. iHUVECs were infected with KSHV for indicated time intervals and expression of CXCR4 was measured by qRT-PCR analysis and normalized to β-*Actin* (housekeeping control). PCR reactions were performed in triplicate and the data presented as mean ΔCT ±SE (CT value of CXCR4-CT value of *β actin)*. Higher ΔCT value indicates lower expression of target gene. (*P<0.05 Student's t-test)
b. Western blot analysis showing a reduction in the level of the CXCR4 protein upon infection of iHUVECs with KSHV.
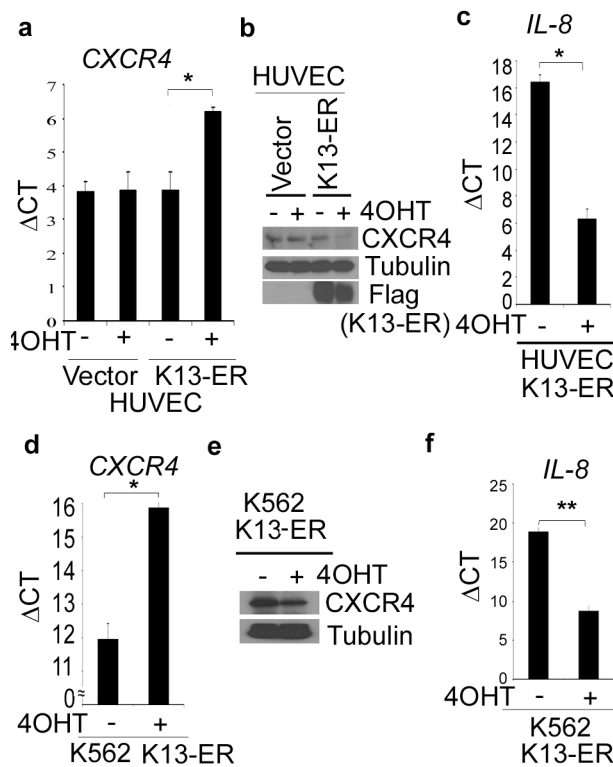
Figure 2. K13 downregulates CXCR4 expression in vascular endothelial cells

a. HUVECs stably expressing a control vector or K13-ER[TAM] were mock-treated or treated with 4OHT (20 nM). After 48 h, RNA was extracted and CXCR4 expression was determined by qRT-PCR. The experiment was performed essentially as described for Figure 1a. (*P<0.05; Student's t- test)

b. Western blot analysis showing a reduction in the level of the CXCR4 protein upon treatment of HUVECs-K13-ER[TAM] with 4OHT.

c. Induction of IL-8 mRNA expression, as measured by qRT-PCR, in HUVECs-K13-ER[TAM] treated with 4OHT. Data is presented as mean   CT±SE as described in Figure 1a. (**P<0.01; Student's t-test)

d. K562 cells stably expressing a control vector or K13-ER[TAM] were mock-treated or treated with 4OHT (20 nM) for 72 h, and expression of CXCR4 mRNA measured by qRT-PCR analysis. (*P<0.05; Student's t- test)

e. Western blot analysis showing a reduction in the level of the CXCR4 protein upon treatment of K562 K13-ER[TAM] cells with 4OHT.

f. Level of IL-8 mRNA expression, as measured by qRT-PCR, in K562-K13-ER[TAM] cells treated with 4OHT. (**P<0.01; Student's t- test).
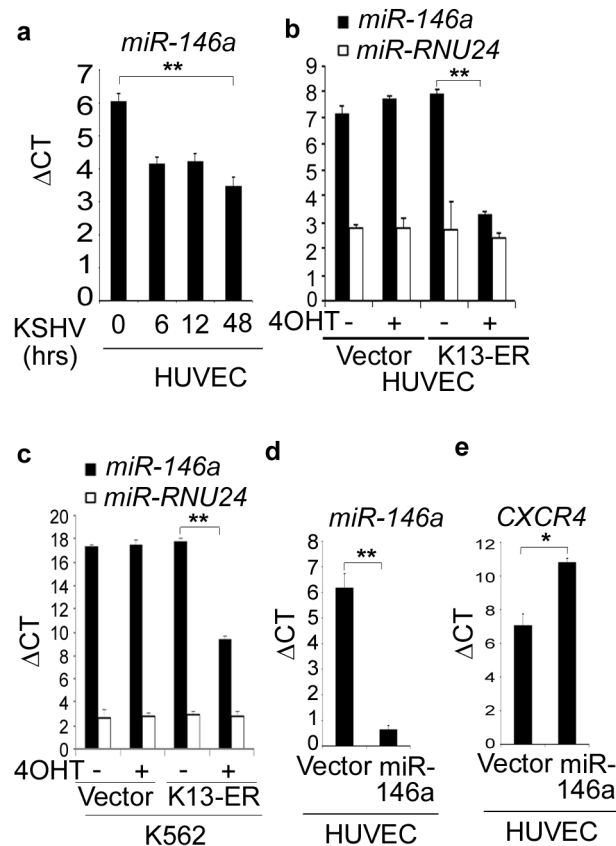
Figure 3. Upregulation of miR-146a expression by KSHV and K13

a. HUVECs were infected with KSHV for 6, 12, and 48 h and expression of miR-146a was measured by Taqman micro RNA assay based qRT-PCR analysis and normalized to miR-RNU48 (housekeeping control). PCR reactions were performed in triplicate and the data presented as mean ΔCT±SE (CT value of miR-146a minus CT value of miR-RNU48). Higher expression is equivalent to smaller ΔCT value. (**P<0.01; Student's t- test).

b-c. K13 upregulates miR-146a expression in HUVECs and K562. HUVECs and K562 cells stably expressing a control vector or K13-ER^{TAM} were mock-treated or treated with 4OHT (20 nM) for 48 h and induction of miR-146a was measured by qRT-PCR. miR-RNU24 was not affected by 4OHT treatment. PCR reactions were performed in triplicate and the data presented as mean ΔCT±SE. (**P<0.01; Student's t- test).

d-e. HUVECs were stably transduced with miR-146a-expressing lentiviral vector and expression of *miR-146a* and CXCR4 was measured by qRT-PCR analysis and normalized to β-*actin* (housekeeping control). qRT-PCR reactions were performed in triplicate and the data presented as mean ΔCT±SE. (*P< 0.05 and **P<0.01; Student's t- test).
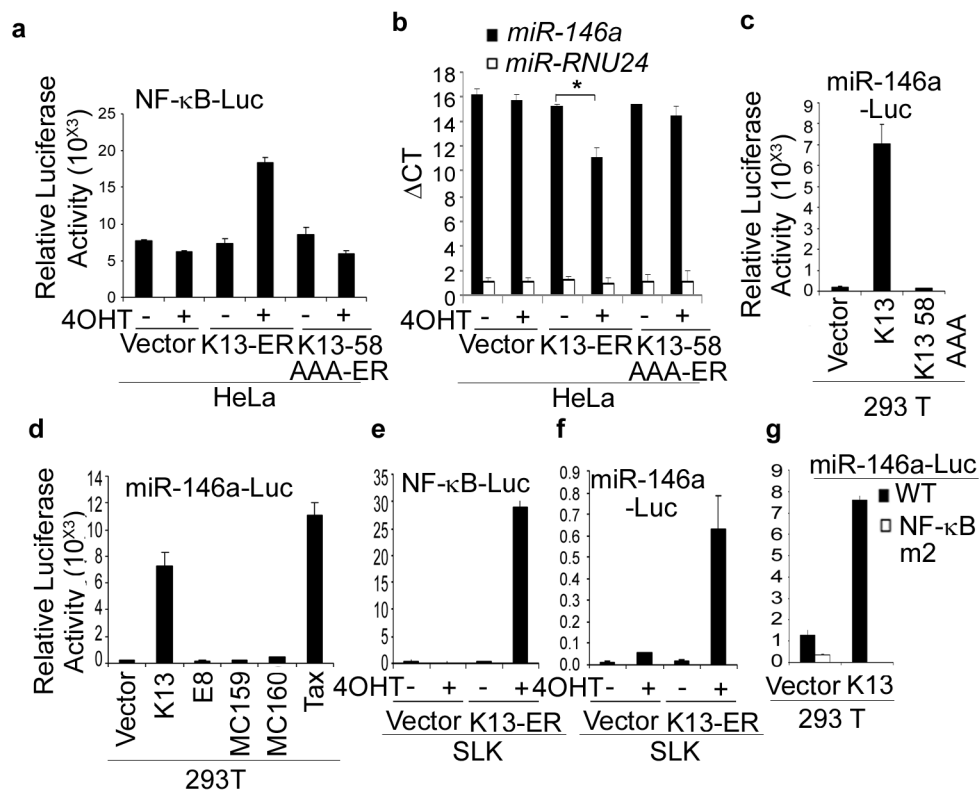
Figure 4. K13 upregulates miR-146a via NF-κB

a. HeLa cells stably expressing a control vector, K13-ER[TAM] or K1358AAA-ER[TAM] were transfected with an NF-κB luciferase reporter construct (75 ng/well) and a *Renilla* reporter construct (75 ng/well) and subsequently treated with 4OHT (20 nM) for 16 h. Luciferase activity was measured as described under Materials and Methods. The values shown are the averages (means±SE) of one representative experiment of three in which each transfection was performed in duplicate.

b. HeLa cells stably expressing a control vector or K13-ER[TAM] or K13 58AAA-ER[TAM] were mock-treated or treated with 4OHT (20 nM) for 48 h and miR-146a expression was measured by qRT-PCR as described for Figure 3b. 4OHT failed to induce miR-146a in HeLa cells expressing an NF-κB-defective mutant of K13 (K13 58AAA-ER[TAM]). K13 has no significant effect on the expression of miR-RNU24, which serves as a negative control.

c. Ectopic expression of wild-type K13 but not its NF-κB defective mutant K13 58AAA induced miR-146a-promoter activity. 293T cells were transfected with an empty vector, wild-type K13 or its NF-κB defective mutant K13 58AAA (250 ng/well) along with a wild-type miR-146a promoter luciferase construct (75 ng/well) and a pRSV/LacZ (galactosidase) reporter construct (75 ng/well), and the reporter assay was performed as described under the Materials and Methods section. The values shown are averages (Mean±SE) of one representative experiment out of three in which each transfection was performed in duplicate.

d. 293T cells were transfected with the indicated vFLIPs (250 ng/well) or HTLV-encoded Tax along with a wild-type miR-146a promoter luciferase construct (75 ng/well) and a

pRSV/LacZ (β-galactosidase) reporter construct (75 ng/well), The experiment was performed essentially as described in Figure 4c

e-f. SLK cells were transfected with a control vector or K13-ER^{TAM} along with an NF-κB luciferase *(e)* reporter construct or miR-146a luciferase reporter *(f)* and a *Renilla* reporter construct (normalization control) and subsequently treated with 4OHT (20 nM) for 48 h. Luciferase activities were measured as described under Materials and Methods. The values shown are the averages (Mean±SE) of one representative experiment of two in which each transfection was performed in duplicate.

g. The two NF-κB sites in the miR-146a promoter are critical for activation by K13. 293T cells were transfected with a control vector or a vector encoding K13 along with either wild-type (miR-146aWT-Luc) or mutant (miR-146a-NF-κBm2-Luc) reporter constructs, and the luciferase reporter assay was performed as described in Figure 4c. The values shown are averages (Mean±SE) of one representative experiments out of three in which each transfection was performed in duplicate.
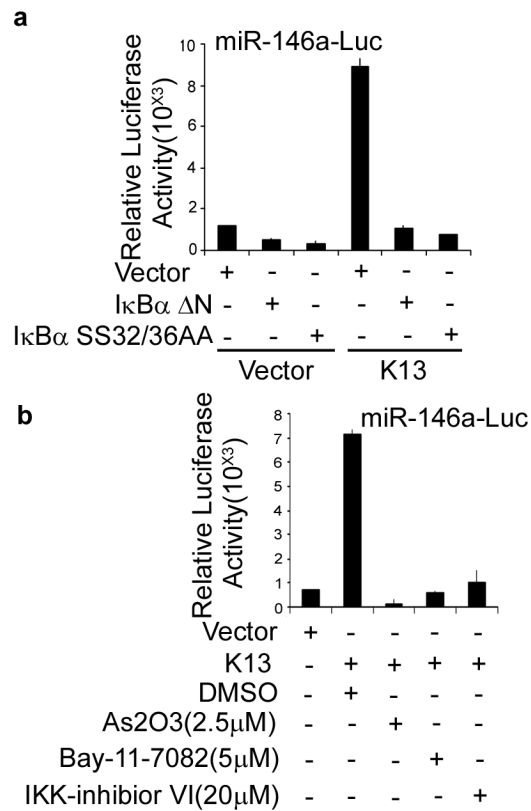
Figure 5. K13 stimulates miR-146a promoter activity via NF-κB activation

a. Dominant-negative mutants of IκBα (IκBα N and IκBαSS32/36AA) block K13-induced miR-146a promoter activity. 293T cells were transfected either with an empty vector or K13, dominant-negative mutants of IκBα along with a miR-146a luciferase reporter construct and a β-galactosidase reporter construct, as described for 4c. The amount of IκBα mutant plasmids (500 ng/well) was five times the amount of vector or K13 (100 ng/well) plasmid, and the total amount of transfected DNA was kept constant by adding empty vector. The values shown are averages (Mean±SE) of one representative experiment out of three in which each transfection was performed in duplicate.

b. Pharmacological inhibitors of NF-κB block K13-induced miR-146a promoter activation. 293T cells were transfected with an empty vector or a vector encoding K13, and subsequently treated with DMSO (vehicle) or the indicated compounds for 16 hours prior to cell lysis. Reporter assay was performed as described for Figure *5a*
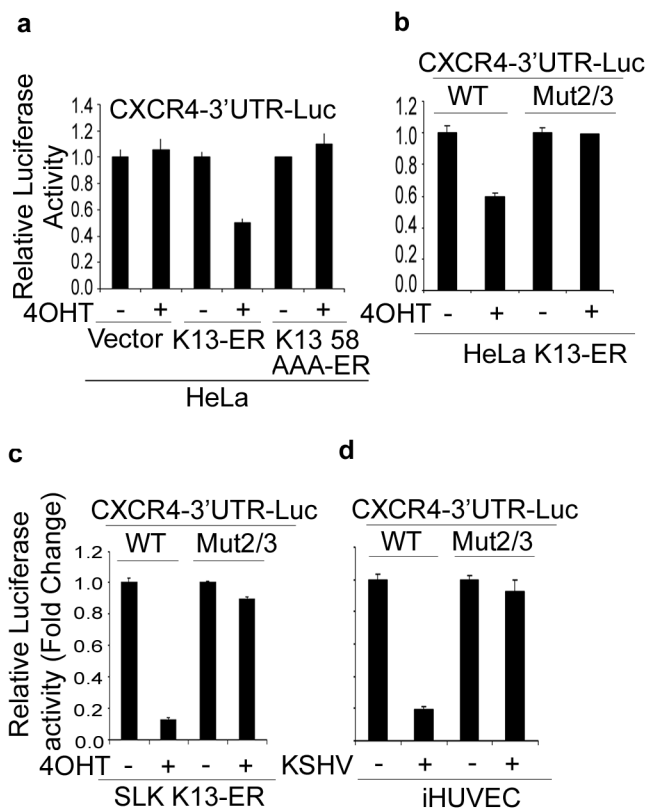
Figure 6. Expression of CXCR4 gene is regulated post-transcriptionally by K13-induced miR-146a

a. HeLa cells stably expressing a control vector, K13-ER[TAM] or K13 58AAA-ER[TAM] were treated with 4OHT (20 nM) for 16 h to induce miR-146a and subsequently transfected with a CXCR4-3′UTR luciferase construct (10 ng/well) and a Renilla reporter construct (75 ng/well). Approximately 48 h later, cell extracts were prepared and reporter assays performed as described in Figure 4a.

b. HeLa cells stably expressing K13-ER[TAM] were treated with 4OHT (20 nM) for 16 h to induce miR-146a and subsequently transfected with a CXCR4-WT-3′UTR luciferase construct or a CXCR4-Mut2/3 3′UTR luciferase construct (10 ng/well) and a *Renilla* reporter construct (75 ng/well). Approximately 48 h later, cell extracts were prepared and reporter assays performed as described in Figure 4a.

c. SLK cells were transfected with K13-ER[TAM] along with a CXCR4-WT 3′UTR or CXCR4-Mut2/3 3′UTR luciferase construct (10 ng/well) and a Renilla reporter construct (75 ng/well) and subsequently treated with 4OHT (20 nM). Approximately 48 h later, cell extracts were prepared and reporter assays performed as described in Figure 4a.

d. iHUVEC cells stably expressing a wild-type CXCR4-3′UTR luciferase construct or Site 2/3 mutated CXCR4-3′UTR luciferase construct were infected with KSHV. Approximately 48 h later, cell extracts were prepared and reporter assays performed as described in Figure 4a.
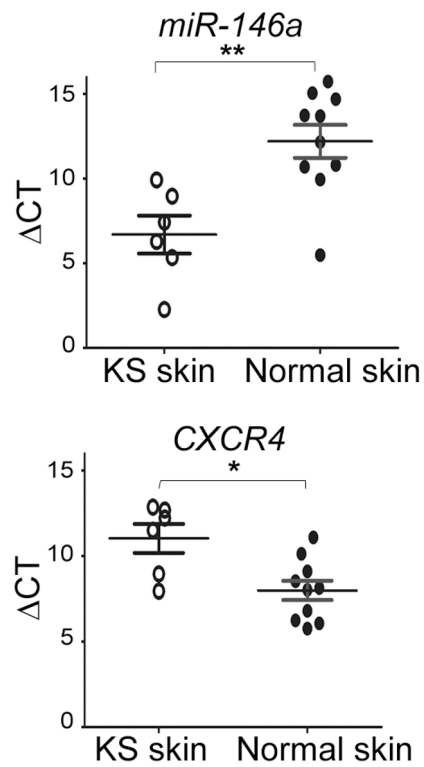
Figure 7. Upregulation of miR-146a and downregulation CXCR4 in KS skin samples
Scatter plot showing normalized ΔCT values in KS skin (n=6) and healthy skin (n=10) patient samples for miR-146a and CXCR4 expression. Open circles and closed indicate KS patient and healthy patient samples, respectively. Horizontal lines represent the mean of normalized ΔCT± SE (*P< 0.05 and **P<0.01; Student's t- test)